Coherent perfect absorption in a quantum nonlinear regime of cavity quantum electrodynamics

Yang-hua Wei,[1] Wen-ju Gu,[1,2] Guoqing Yang,[1,3] Yifu Zhu,[4] and Gao-xiang Li[1,*]

[1]*Department of Physics, Huazhong Normal University, Wuhan 430079, China*

[2]*School of Physics and Optoelectronic Engineering, Yangtze University, Jinzhou 434023, China*

[3]*School of Electronics and Information, Hangzhou Dianzi University, Hangzhou 310018, China*

[4]*Department of Physics, Florida International University, Miami, Florida 33199, USA*

(Received 24 October 2017; published 18 May 2018)

Coherent perfect absorption (CPA) is investigated in the quantum nonlinear regime of cavity quantum electrodynamics (CQED), in which a single two-level atom couples to a single-mode cavity weakly driven by two identical laser fields. In the strong-coupling regime and due to the photon blockade effect, the weakly driven CQED system can be described as a quantum system with three polariton states. CPA is achieved at a critical input field strength when the frequency of the input fields matches the polariton transition frequency. In the quantum nonlinear regime, the incoherent dissipation processes such as atomic and photon decays place a lower bound for the purity of the intracavity quantum field. Our results show that under the CPA condition, the intracavity field always exhibits the quadrature squeezing property manifested by the quantum nonlinearity, and the outgoing photon flux displays the super-Poissonian distribution.

DOI: 10.1103/PhysRevA.97.053825

I. INTRODUCTION

Control of photon absorption, scattering, and localization is a current research topic in optical physics and has been extensively investigated in both theories and experiments [1–5]. Recently, coherent perfect absorption (CPA) that arises from the interference of two counterpropagating light fields in a confined cavity structure has attracted considerable interest and may have potential applications in optical logical devices, energy storage, information communication, and acoustic absorption [6]. CPA has been studied in solid Fabry-Perot etalons containing a loss medium [1,2], subwavelength thin films [7–12], planar slab [13,14], metamaterials [15–18], and waveguides [19,20]. The applications of CPA have been explored in graphene [21–24], photonic structures [25–29], resonators [30], and other complex-structure devices [31–34]. Most CPA studies are carried out in the linear optical regime and the CPA systems are treated classically [1,7–31]. Some recent studies of CPA have been extended to the nonlinear optical regime. For example, the nonlinear CPA has been investigated in a Helmholtz resonator [35] and a distributed Bragg reflector [36]. Based on a semiclassical model, CPA has been studied recently in a cavity quantum electrodynamics (CQED) system consisting of N two-level atoms confined in a single-mode cavity. The results show that CPA can be readily observed in both the linear and nonlinear excitation regime when the CQED system satisfies the strong collective coupling condition [37,38]. In addition, the CQED system consisting of N three-level atoms also demonstrates the feasibility of interference control of perfect photon absorption in linear excitation regimes [39].

All previous studies of CPA are done on optical system with multiple absorbers and classical light fields. One can argue that with a large optical depth of the absorber, the input light can essentially be completely absorbed, thus making the CPA less useful for applications. However, if one can manipulate the atom-photon coupling and ultimately realize the ideal condition in which a single photon can be absorbed with a 100% probability, it will provide a new insight for studies of quantum nonlinear optics and its applications. It was well known that for a single-atom CQED system in the strong-coupling regime of the atom-photon interaction, a photon can be converted into the atomic excitation with a high probability through the polariton excitation. Distinct from the previous theoretical and experimental investigations on photon trapping in single-atom CQED systems with one-sided driving [40–43], here we present a fully quantized analysis of CPA in a CQED system consisting of a single two-level atom coupled to a single-cavity mode with the use of two-sided driving fields, and show that statistically CPA can be achieved in the strong-coupling regime. Thus the CQED with CPA fulfills the ideal goal of the atom-photon interaction: a single photon is completely absorbed by a single atom, or the photonic excitation with a single photon is converted into the atomic excitation of a single atom with a 100% probability.

In the semiclassical treatment of CPA in the CQED system with N two-level atoms via ignoring the quantum correlations, the intracavity light is treated as a coherent field, and the nonlinear CPA is induced by the destructive interference between the intracavity field and input fields [38]. However, in the quantum nonlinear regime of the CQED study presented here, the dissipation processes decrease the coherence of the intracavity field, and the interference between the coherent input fields is different from that of the semiclassical analysis. Using the secular approximation, we derive the analytical expression of the output field from the cavity and show that the

*gaox@mail.ccnu.edu.cn

average amplitude of output field is nonlinearly dependent on the input field. The CPA is realized in the nonlinear regime of the CQED when the input laser fields match a critical intensity and are resonant with the polariton transition. The nonlinearity considered here is induced by the polariton excitation of the CQED system, which is negligible in the linear CPA in a multiatom CQED system. We also show that the incoherent processes, such as atomic and cavity dissipations of excited polariton states, reduce the coherence of the intracavity field and place a lower bound on the purity of the intracavity field. The quantum nonlinearity can also generate nonclassical statistical properties such as the quadrature squeezing of the intracavity field. We discuss the higher-order correlation function and show that the coherent part of the intracavity field can interfere with the input light, leading to a null average amplitude, but the fluctuation of the output field is still nonzero due to the mixed state of the intracavity field under the condition of CPA.

The paper is organized as follows. In Sec. II, the CQED system is introduced; in Sec. III, the generation of CPA in the quantum nonlinear regime is analyzed; in Sec. IV, the quadrature squeezing of the intracavity field and the properties of the output field are presented; and in Sec. V, the conclusion is presented.

II. THE DESCRIPTION OF CQED SYSTEM

A typical CQED system is shown in Fig. 1, in which a two-level atom couples to a cavity consisting of two high-reflectivity mirrors that is driven by two laser fields $a^l_{\rm in}$ and $a^r_{\rm in}$ (with the same frequency $\nu_l = \nu_r = \nu$) from two opposite sides, respectively. In the rotating frame of the input laser frequency, the system Hamiltonian

$$H = -\delta a^\dagger a - \frac{\Delta}{2}(\sigma^\dagger\sigma - \sigma\sigma^\dagger) + g(\sigma^\dagger a + a^\dagger\sigma) + i\left(a^r_{\rm in}\sqrt{\frac{\kappa_r}{\tau}} + a^l_{\rm in}\sqrt{\frac{\kappa_l}{\tau}}\right)(a^\dagger - a), \quad (1)$$

where a is the annihilation operator of cavity mode, σ is the atomic transition operator, $\delta = \nu_l - \nu_{\rm cav}$ is the detuning between the laser frequency ν_l and cavity frequency $\nu_{\rm cav}$, and $\Delta = \nu_l - \nu_{\rm eg}$ is the detuning between the laser frequency ν_l and atomic frequency $\nu_{\rm eg}$. The atom-cavity coupling strength is g, and the coupling coefficient of the input laser fields and the cavity mode is $\sqrt{\kappa_i/\tau}$ $(i = l,r)$, with the loss rate κ_i related to the mirror transmission T_i and photon round-trip time inside the cavity τ by $\kappa_i = T_i/\tau$. We consider a symmetric arrangement such that $T_l = T_r = T$, and then $\kappa_l = \kappa_r = \kappa$, the total cavity decay rate 2κ.

The evolution of system is described by the master equation

$$\dot\rho = -i[H,\rho] + \mathcal{L}_c\rho + \mathcal{L}_a\rho, \quad (2)$$

in which the loss of cavity mode and atomic dissipation are described by the Lindblad operators

$$\mathcal{L}_c\rho = \kappa(2a\rho a^\dagger - \rho a^\dagger a - a^\dagger a\rho),$$
$$\mathcal{L}_a\rho = \Gamma(2\sigma\rho\sigma^\dagger - \rho\sigma^\dagger\sigma - \sigma^\dagger\sigma\rho), \quad (3)$$

with the atomic dissipation rate 2Γ.

The output fields of the cavity from the two ports are determined by the input-output equations

$$a^l_{\rm out} = \sqrt{T}a - a^l_{\rm in}, \quad a^r_{\rm out} = \sqrt{T}a - a^r_{\rm in}. \quad (4)$$

If the average amplitudes of output fields from the two ports are equal to zero, the input lasers are completely absorbed by CQED system, and CPA occurs [2,44].

III. GENERATION OF NONLINEAR CPA IN THE SINGLE-PHOTON QUANTUM REGIME

Strong atom-cavity coupling in CQED is achievable in single-atom or ion CQED systems [41,45,46], as well as artificial atom systems such as quantum dots [47] and defect centers [48]. The anharmonic energy-ladder structure is formed in such CQED systems. When the cavity excitation rate is much smaller than the atom-cavity coupling strength, the system can be well treated approximately in the single-photon excitation space due to the effect of the photon blockade at the appropriate frequency of the driving laser fields. Thus, the system can be excited from the ground state $|0\rangle = |g,0\rangle$ only to the first excited manifold $\{|e,0\rangle, |g,1\rangle\}$, when the frequency of the driving laser fields is tuned near the transition frequency of the first-order polariton states that are formed by strong atom-cavity coupling as shown in Fig. 2.

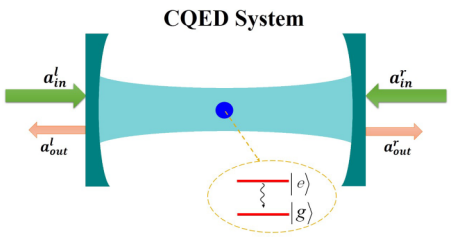

FIG. 1. A typical CQED system consisting of a two-level atom coupled to a two-sided cavity mode. The atom is strongly coupled to the cavity mode, and the cavity mode is driven by two coherent laser fields, $a^l_{\rm in}$ and $a^r_{\rm in}$, with the same frequency and amplitude from the two ports.

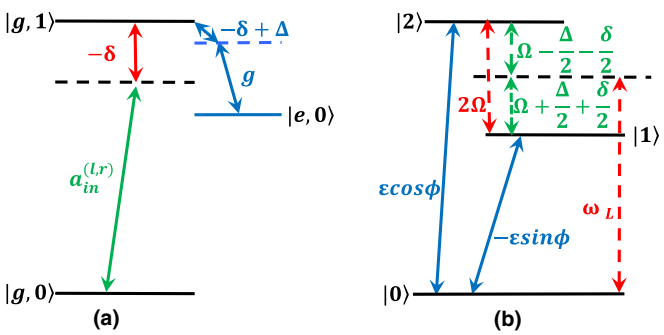

FIG. 2. (a) Level structure of the CQED system confined within the single-excitation states due to the effect of the photon blockade in the strong atom-cavity coupling regime. (b) Transitions between the polariton states formed by the hybridizing atom and cavity modes due to the strong atom-cavity coupling.

A. Theoretical investigation of CPA in the polariton states

Under the condition of strong atom-cavity coupling $g \gg \{\kappa,\Gamma,-\delta+\Delta\}$, the polariton states of hybridizing the atom and cavity modes are formed as

$$\begin{aligned}|1\rangle &= \cos\phi|e,0\rangle - \sin\phi|g,1\rangle,\\ |2\rangle &= \sin\phi|e,0\rangle + \cos\phi|g,1\rangle,\end{aligned} \tag{5}$$

where $\sin\phi = \sqrt{\frac{2\Omega-\Delta+\delta}{4\Omega}}$, $\cos\phi = \sqrt{\frac{2\Omega+\Delta-\delta}{4\Omega}}$, $\Omega = \sqrt{g^2+(\frac{\Delta-\delta}{2})^2}$, and the energy frequencies are $-2\delta \mp \Omega$. Then the CQED system can be approximately treated as a three-level quantum system consisting of one ground state $|0\rangle$ and two excited states $|1\rangle$ and $|2\rangle$, as shown in Fig. 2(b). In such polariton states, the cavity and atomic operators can be rewritten as

$$\begin{aligned}a &= -\sin\phi|0\rangle\langle 1| + \cos\phi|0\rangle\langle 2|,\\ \sigma &= \cos\phi|0\rangle\langle 1| + \sin\phi|0\rangle\langle 2|,\end{aligned} \tag{6}$$

and the Hamiltonian of this CQED system becomes

$$\begin{aligned}H = {}& \frac{\Delta}{2}|0\rangle\langle 0| + \left(-\frac{\delta}{2}-\Omega\right)|1\rangle\langle 1| + \left(-\frac{\delta}{2}+\Omega\right)|2\rangle\langle 2|\\ &+ i\varepsilon(-\sin\phi|1\rangle\langle 0| + \cos\phi|2\rangle\langle 0| + \sin\phi|0\rangle\langle 1|\\ &- \cos\phi|0\rangle\langle 2|),\end{aligned} \tag{7}$$

where $\varepsilon = \sqrt{\frac{\kappa}{\tau}}(a_{\rm in}^l + a_{\rm in}^r)$. Under the assumption of symmetrical laser inputs $a_{\rm in}^l = a_{\rm in}^r = a_{\rm in}$, the total driving strength becomes $\varepsilon = 2\sqrt{\frac{\kappa}{\tau}}a_{\rm in}$.

Taking into account cavity and atomic dissipations, the density-matrix elements obey the following set of coupled differential equations:

$$\begin{aligned}\dot{\rho_{00}} &= \varepsilon\rho_{10}\sin\phi - \varepsilon\rho_{02}\cos\phi + \varepsilon\rho_{01}\sin\phi - \varepsilon\rho_{20}\cos\phi + 2(\kappa\cos^2\phi + \Gamma\sin^2\phi)(\rho_{11}+\rho_{22}),\\ \dot{\rho_{01}} &= \left[-i\left(\frac{\Delta}{2}+\frac{\delta}{2}+\Omega\right) - (\kappa\sin^2\phi + \Gamma\cos^2\phi)\right]\rho_{01} - \varepsilon\rho_{00}\sin\phi + \varepsilon\rho_{11}\sin\phi - \varepsilon\rho_{21}\cos\phi,\\ \dot{\rho_{02}} &= \left[-i\left(\frac{\Delta}{2}+\frac{\delta}{2}-\Omega\right) - (\kappa\cos^2\phi + \Gamma\sin^2\phi)\right]\rho_{02} + \varepsilon\rho_{00}\cos\phi + \varepsilon\rho_{12}\sin\phi - \varepsilon\rho_{22}\cos\phi,\\ \dot{\rho_{11}} &= -2(\kappa\sin^2\phi + \Gamma\cos^2\phi)\rho_{11} - \varepsilon\rho_{01}\sin\phi - \varepsilon\rho_{10}\sin\phi,\\ \dot{\rho_{12}} &= [2i\Omega - (\kappa+\Gamma)]\rho_{12} - \varepsilon\rho_{02}\sin\phi + \varepsilon\rho_{10}\cos\phi,\\ \dot{\rho_{22}} &= -2(\kappa\cos^2\phi + \Gamma\sin^2\phi)\rho_{22} + \varepsilon\rho_{02}\cos\phi + \varepsilon\rho_{20}\cos\phi.\end{aligned} \tag{8}$$

With appropriate chosen values of Δ, δ, and Ω, the states $|0\rangle$ and $|2\rangle$ are near resonant, i.e., the frequency detunings $\frac{\Delta}{2}+\frac{\delta}{2}-\Omega$ close to the linewidth $\kappa\sin^2\phi + \Gamma\cos^2\phi$. While in the regime of strong coupling ($2\Omega \gg \{\kappa,\Gamma\}$) and weak driving ($\{2\Omega,\kappa\} \gg \varepsilon$), transitions $|0\rangle \to |1\rangle$ and $|1\rangle \to |2\rangle$ are far off-resonance since the detuning is about 2Ω. Therefore, it is feasible to apply the secular approximation by setting off-resonant terms ρ_{10}, ρ_{11}, ρ_{12}, and ρ_{21} approximately equal to zero. Then evolution equations of density matrix elements can be simplified to only concern the states of $|0\rangle$ and $|2\rangle$, and the solutions in the long-time limit are in the form

$$\rho_{02} = \frac{\sqrt{T^{-1}}}{A_0}[8(\kappa\cos^2\phi + \Gamma\sin^2\phi)\kappa a_{\rm in}\cos\phi - 4i(\Delta+\delta-2\Omega)\kappa a_{\rm in}\cos\phi], \tag{9}$$

$$\rho_{22} = \frac{16\kappa^2 a_{\rm in}^2 T^{-1}\cos^2\phi}{A_0}, \tag{10}$$

$$\rho_{00} = \frac{1}{A_0}[4(\kappa\cos^2\phi + \Gamma\sin^2\phi)^2 + 16\kappa^2 a_{\rm in}^2 T^{-1}\cos^2\phi + (\Delta+\delta-2\Omega)^2], \tag{11}$$

where $A_0 = 4(\kappa\cos^2\phi + \Gamma\sin^2\phi)^2 + (\Delta+\delta-2\Omega)^2 + 32\kappa^2 a_{\rm in}^2 T^{-1}\cos^2\phi$, and T is the transmittance of the mirror. The average value of operator a becomes

$$\langle a\rangle = \frac{a_{\rm in}\sqrt{T^{-1}}}{A_0}[8(\kappa\cos^2\phi + \Gamma\sin^2\phi)\kappa\cos^2\phi + 4i(\Delta+\delta-2\Omega)\kappa\cos^2\phi]. \tag{12}$$

And the average value of number-operator $\langle N\rangle = \rho_{22}\cos^2\phi = 16\kappa^2 a_{\rm in}^2 T^{-1}\cos^4\phi/A_0$, where $N = a^\dagger a$.

From the input-output relation in Eq. (4) the output fields of two mirrors are equal and are given by

$$\frac{\langle a_{\rm out}\rangle}{a_{\rm in}} = \frac{(\kappa^2\cos^4\phi - \Gamma^2\sin^4\phi) - 8\kappa^2 a_{\rm in}^2 T^{-1}\cos^2\phi - \left(\frac{\Delta}{2}+\frac{\delta}{2}-\Omega\right)^2 + 2i\left(\frac{\Delta}{2}+\frac{\delta}{2}-\Omega\right)\kappa\cos^2\phi}{(\kappa\cos^2\phi + \Gamma\sin^2\phi)^2 + 8\kappa^2 a_{\rm in}^2 T^{-1}\cos^2\phi + \left(\frac{\Delta}{2}+\frac{\delta}{2}-\Omega\right)^2}. \tag{13}$$

Equation (13) shows the nonlinear dependence on the input field. The nonlinear relation indicates that the three-level CQED model presented here is beyond the weak excitation limit. In the weak excitation limit, the excitation is negligible

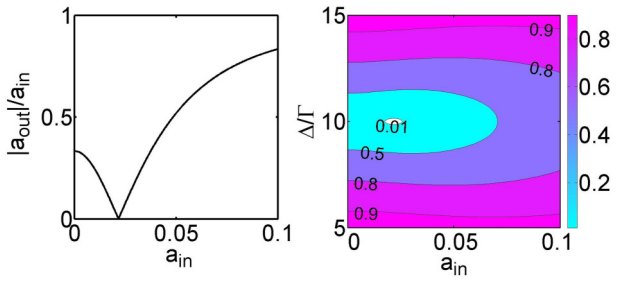

FIG. 3. The output fields from the output ports which are equal and scaled by the input field versus (a) the amplitude of input field $a_{\rm in}$ and (b) the detuning Δ/Γ and amplitude of input field $a_{\rm in}$, with the parameters $\kappa = 2\Gamma$, $g = 10\Gamma$, $\Delta = \delta$, and $T = 0.01$.

and $\rho_{00} = 1$, and then the output field $\langle a_{\rm out}\rangle/a_{\rm in} = \frac{\kappa\Delta-\Gamma\delta}{\kappa\Delta+\Gamma\delta}$. The conditions of perfect photon absorption are $\kappa\Delta = \Gamma\delta$, which is consistent with the linearized result derived semiclassically for the multiatom CQED system in Ref. [37]. When the excitation of the upper levels is included, the output field becomes nonlinearly dependent on the input field. The perfect absorption occurs when the following conditions are met:

$$\Delta\delta = g^2, \tag{14a}$$

$$a_{\rm in}^2 = \frac{T(\kappa^2\Delta^2 - \Gamma^2\delta^2)}{8\kappa^2\Delta(\Delta+\delta)}. \tag{14b}$$

The first relation requires that the input laser fields are resonant to the transition $|0\rangle \rightarrow |2\rangle$ shown in Fig. 2(b), and the second condition gives the required strength of input laser fields for the CPA. The CPA appears only at a given input field strength, which is a characteristic of the nonlinear dynamics. In Fig. 3(a) we show the dependence of the output field on the input field which reveals the difference from the linear CPA that is independent of the input field strength [37]. Figure 3(b) presents a two-dimensional (2D) contour plot demonstrating that CPA can only occur when both the strength and the frequency of the input fields satisfy Eq. (14).

In the quantum nonlinear CPA, the polariton excitation is taken into account, and thus the photon scattered by the system is the mixed state due to dissipation processes involved. The underlying physics of the CPA can be further clarified when the purity of the CQED states is analyzed.

B. The quantum nonlinear CPA limited by the intracavity coherence

The underlying physics of CPA is the destructive interference between the intracavity field and the coherent input field [2]. In the linearized approach [37], the atomic population is in the ground state, atomic excitation is ignorable, and quantum dissipation processes do not play a role there. However for the quantum CPA analysis presented here, the excitation in state $|2\rangle$ becomes

$$\rho_{22} = \frac{\kappa\Delta - \Gamma\delta}{4\kappa\Delta}, \tag{15}$$

which is 0.125 when $\kappa\Delta = 2\Gamma\delta$. Now the incoherent processes of the excited state, such as spontaneous atomic decay and dissipation of cavity photons into free-space photons, should be included. The incoherent processes will decrease the coherence of the intracavity field and also influence the destructive interference which requires the coherence.

To evaluate the influence of incoherent processes on CPA, we analyze the purity of the intracavity photon state,

$$\mathrm{Tr}(\rho^2) = (1 - \rho_{22}\cos^2\phi)^2 + 2|\rho_{02}|^2\cos^2\phi + \rho_{22}^2\cos^4\phi, \tag{16}$$

from which it is evident that $\mathrm{Tr}(\rho^2) = 1$ for the pure state of intracavity photon state. The purity takes the minimum value

$$\mathrm{Tr}(\rho^2)_{\rm min} = \frac{7\Delta^2 + 14\Delta\delta + 8\delta^2}{8(\Delta+\delta)^2}, \tag{17}$$

under the condition of $a_{\rm in}^2 = \frac{T(\kappa\Delta+\Gamma\delta)^2}{8\kappa^2\Delta(\Delta+\delta)}$. Meanwhile, the average of operator a takes the maximum value $\langle a\rangle_{\rm max} = \sqrt{\frac{\Delta}{8(\Delta+\delta)}}$, with $\langle a^\dagger a\rangle = \frac{\Delta}{4(\Delta+\delta)}$, which fulfills the relation $2|\langle a\rangle_{\rm max}|^2 = \langle a^\dagger a\rangle$. Furthermore, the inequality $2|\langle a\rangle|^2 > \langle a^\dagger a\rangle$ will be achieved when $a_{\rm in}^2 < \frac{T(\kappa\Delta+\Gamma\delta)^2}{8\kappa^2\Delta(\Delta+\delta)}$, which is a necessary and sufficient condition of squeezing of the intracavity field comprised by the superposition of Fock states $|0\rangle$ and $|1\rangle$ [49,50]. Explicitly, when $\Delta = \delta$, $\mathrm{Tr}(\rho^2)_{\rm min} = \frac{29}{32} \approx 0.906$, $\langle a\rangle_{\rm max} = \frac{1}{4}$, $\langle a^\dagger a\rangle = \frac{1}{8}$, and $a_{\rm in}^2 = \frac{T}{16}$.

Moreover, under the CPA conditions of Eqs. (14), the purity becomes

$$\mathrm{Tr}(\rho^2)_{\rm CPA} = 1 - \frac{\Delta(\Delta+2\delta)}{2(\Delta+\delta)^2}\left(\frac{1}{2} - \frac{\Gamma\delta}{2\kappa\Delta}\right)^2. \tag{18}$$

With the requirement of positive value of $a_{\rm in}^2$, $\Gamma\delta/\kappa\Delta$ should fulfill the value range (0,1). When $\Gamma\delta = \kappa\Delta$, the input field $a_{\rm in} = 0$, the system is in the linearized regime, and the purity becomes unity, where the incoherent processes are not involved. $\mathrm{Tr}(\rho^2)_{\rm CPA} = \mathrm{Tr}(\rho^2)_{\rm min}$ in the limit $\Gamma\delta \ll \kappa\Delta$, which means the atomic dissipation is ignored. Otherwise, $\mathrm{Tr}(\rho^2)_{\rm CPA} > \mathrm{Tr}(\rho^2)_{\rm min}$. Therefore, if we intend to achieve the CPA, the purity should never drop below the threshold purity value. Because of the interference of the Fock states, the intracavity photon is in a squeezing state, showing nonclassical properties under CPA, which is in the next section.

The physical process behind the quantum nonlinear CPA is the match between the coherent part of the intracavity field and the coherent input fields. When $\Delta = \delta$, the required input field for CPA becomes $a_{\rm in}^2 = T[1 - (\Gamma/\kappa)^2]/16$. Therefore, the increase of two-sided inputs is associated with the increase of intracavity photons but also the decrease of purity. When the coherent part of the intracavity field can match with the left (or right) input field at the certain value, the nonlinear quantum CPA occurs. However, when the purity is below the critical value, such as $\mathrm{Tr}(\rho^2)_{\rm min}$ as discussed above, the coherence of the intracavity field cannot match the input field, and the quantum nonlinear CPA disappears. Thus, due to the nonlinear dependence and negative correlation between the purity and the inputs, there exists an upper limit of the inputs that specifies the lowest limit of purity.

The incoherence will affect the CPA and vice versa. In Fig. 4 we plot the purity versus detuning Δ. In the vicinity of CPA ($\Delta = g$), there exists a peak which indicates the increase of coherence due to CPA.

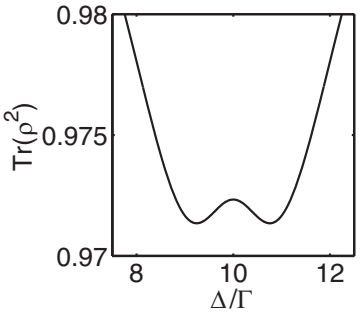

FIG. 4. The purity of the intracavity field versus the detuning Δ/Γ with the parameters $\kappa = 2\Gamma$, $g = 10\Gamma$, $\Delta = \delta$, $T = 0.01$, and $a_{\rm in} = 0.0216$ [determined by the CPA condition in Eq. (14)].

IV. THE SQUEEZING OF AN INTRACAVITY PHOTON WITH QUANTUM NONLINEAR CPA

To generate the nonclassical properties of the photon field, Wódkiewicz *et al.* suggested to utilize the interference effect of superposition of Fock states and ignore dissipation. They had obtained maximum squeezing on some time points under different initial states of $|0\rangle$, $|1\rangle$, and $|2\rangle$ through the Jaynes-Cummings model [49]. Haroche has experimentally measured the negative value of the Wigner function with a zero- and one-photon field using the Lutterbach-Davidovich method [51]. Recently, Duan has proposed and experimentally demonstrated the nonclassical properties using the superposition of Fock states $|0\rangle$ and $|N\rangle$ [52]. Due to the effect of photon blockade, the intracavity field is confined within one excitation, and according to the mechanism of generating squeezing by coherently superposing Fock states $|0\rangle$ and $|1\rangle$ [49,53,54], here we discuss the squeezing property of the intracavity field and especially discuss the optimal squeezing at the CPA conditions. The quadrature components X_1 and X_2 of the intracavity field are defined as

$$X_1 = \frac{1}{\sqrt{2}}(ae^{-i\theta/2} + a^\dagger e^{i\theta/2}),$$
$$X_2 = \frac{1}{\sqrt{2}i}(ae^{-i\theta/2} - a^\dagger e^{i\theta/2}), \tag{19}$$

where θ is the phase angle. If the quadrature variance $\langle(\Delta X_1)^2\rangle < 1/2$ or $\langle(\Delta X_2)^2\rangle < 1/2$, the intracavity field is squeezed.

The variance of X_1 is

$$\langle(\Delta X_1)^2\rangle = \tfrac{1}{2} + (\rho_{22} - |\rho_{02}|^2)\cos^2\phi - \tfrac{1}{2}\left(\rho_{20}^2 e^{-i\theta} + \rho_{02}^2 e^{i\theta}\right)\cos^2\phi. \tag{20}$$

When the phase angle $\theta/2 = \arg(\rho_{20})$, the variance becomes $\langle(\Delta X_1)^2\rangle = \frac{1}{2} + (\rho_{22} - 2|\rho_{02}|^2)\cos^2\phi$, and if $2|\rho_{02}|^2 > \rho_{22}$ is satisfied, the intracavity is squeezed. Under the condition of CPA, $2|\rho_{02}|^2 = \rho_{22}\frac{\kappa\Delta+\Gamma\delta}{\kappa\Delta}$, and thus the intracavity field is always squeezed. To achieve the optimal squeezing under the conditions of CPA, we should further simplify the variance as

$$\langle(\Delta X_1)^2\rangle = \frac{1}{2} + \frac{1}{4}\left[\left(\frac{\Gamma\delta}{\kappa\Delta}\right)^2 - \left(\frac{\Gamma\delta}{\kappa\Delta}\right)\right]\frac{\Delta}{\Delta+\delta}, \tag{21}$$

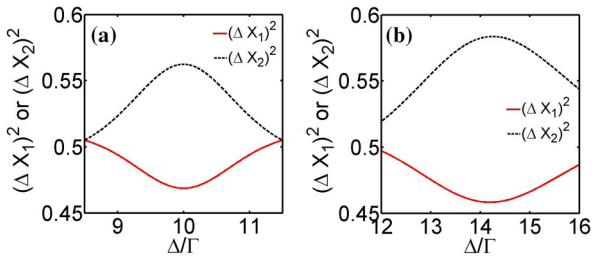

FIG. 5. (a) The squeezing of the intracavity field versus the detuning Δ/Γ with the resonance of cavity mode and atomic transition ($\Delta = \delta$), and the other parameters $\kappa = 2\Gamma$, $g = 10\Gamma$, $T = 0.01$, and $a_{\rm in} = 0.0216$ [determined by the CPA condition in Eq. (14)]. (b) The squeezing of the intracavity field versus the detuning Δ/Γ with cavity mode blue-detuned to atomic transition ($\Delta = 2\delta = 14.14\Gamma$), and the other parameters $\kappa = \Gamma$, $g = 10\Gamma$, $T = 0.01$, and $a_{\rm in} = 0.025$ [determined by the CPA condition in Eq. (14)].

which can be maximized by requiring $\Gamma\delta = \kappa\Delta/2$, which leads to $\langle(\Delta X_1)^2\rangle = \frac{1}{2} - \frac{1}{16}\frac{\Delta}{\Delta+\delta}$. The maximum squeezing is 0.58 dB. When the cavity field is resonant to atomic transition, i.e., $\Delta = \delta$, we have $\kappa = 2\Gamma$ and the variance is 0.468, as shown in Fig. 5(a), which corresponds to 0.28 dB squeezing. Moreover, when the cavity field is tuned off resonance from the atomic transition $\delta' = \Delta - \delta = \nu_{\rm cav} - \nu_{21}$, the better squeezing is achieved when the cavity field is blue-detuned from atomic transition at $\nu_{\rm cav} > \nu_{21}$ ($\delta' > 0$). For example, for symmetric damping rates $\kappa = \Gamma$, we have $\Delta - \delta = 5\sqrt{2}\Gamma$ with $g = 10\Gamma$, and the variance is 0.458, as shown in Fig. 5(b), which corresponds to 0.38 dB squeezing.

For the blue-detuning $\delta' > 0$, the photonic excitation takes a larger ratio of the polariton excitation, as shown in Fig. 6(b), and the intracavity field will show strong nonlinearity from the polariton excitation, which could improve the squeezing. The condition is realizable in the photon blockade system of a single ^{87}Rb atom-cavity CQED [42], where the atomic dissipation rate is $\Gamma/2\pi = 3$ MHz, the cavity decay rate is $\kappa/2\pi = 2$ MHz, and the coupling strength is $g/2\pi \approx 20$ MHz. When we choose the detuning $\delta' = 7.7\Gamma$, from the CPA conditions in Eq. (14) we have $\delta = 3.85\Gamma$, $\Delta = 11.55\Gamma$, and input field $a_{\rm in} = 0.0265$. The variance is 0.453 and the squeezing is 0.43 dB, as shown in Fig. 6(a).

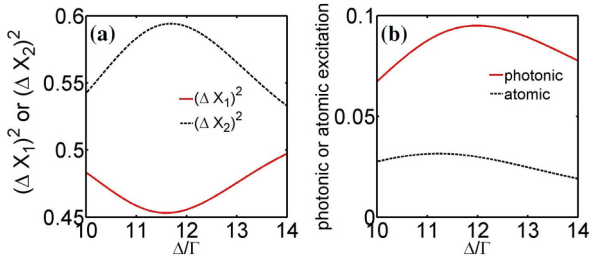

FIG. 6. (a) The squeezing of the intracavity field versus the detuning Δ/Γ with cavity mode blue-detuned to atomic transition ($\Delta - \delta = 7.7\Gamma$), and the other parameters $\kappa = 2/3\Gamma$, $g = 20/3\Gamma$, $T = 0.01$, and $a_{\rm in} = 0.0265$ [determined by the CPA condition in Eq. (14)]. (b) The photonic or atomic excitation versus the detuning Δ/Γ with cavity mode blue-detuned to atomic transition.

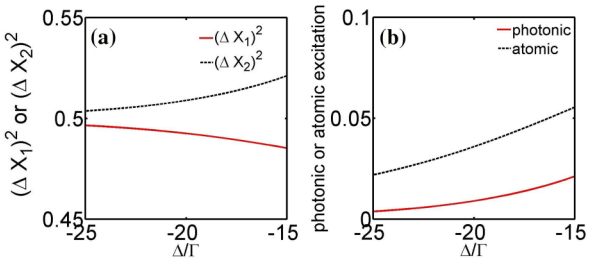

FIG. 7. (a) The squeezing of the intracavity field versus the detuning Δ/Γ with cavity mode red-detuned to atomic transition ($\Delta - \delta = -15\Gamma$), and the other parameters $\kappa = 10\Gamma$, $g = 10\Gamma$, $T = 0.01$, and $a_{\rm in} = 0.0316$ [determined by the CPA condition in Eq. (14)]. (b) The photonic or atomic excitation versus the detuning Δ/Γ with cavity mode red-detuned to atomic transition.

In contrast, for the red-detuning $\delta' = \Delta - \delta < 0$, the atomic excitation takes a larger ratio of the polariton excitation, as shown in Fig. 7(b), and intracavity nonlinearity is deceased, which could reduce the squeezing. If we choose the detuning $\delta' = -15\Gamma$, we have $\delta = -5\Gamma$, $\Delta = -20\Gamma$, $\kappa = 20\Gamma$, and input field $a_{\rm in} = 0.0316$. The squeezing effect is smaller at $\Delta = -20\Gamma$ compared with the blue-detuning, $\delta' = \Delta - \delta > 0$, which corresponds to occurrence of CPA, as shown in Fig. 7(a).

Finally, we show the distinctions between the quantum nonlinear CPA and semiclassical nonlinear CPA [38] and the linear CPA [37]. For the semiclassical nonlinear CPA, the quantum fluctuations do not play a role because the intracavity photon is treated as a classical coherent field and the variance, $\langle(\Delta a_{\rm out})^2\rangle = 0$. However, in the quantum analysis, the dissipation of polariton excitation can reduce the coherence, leading to the mixed intracavity field, and the interference between the mixed state and the coherent inputs is not complete. Typically, the phenomenon of CPA deals with the average of interference between the intracavity field and coherent inputs, which is semiclassical in its essence. The characteristics of quantum from classical is represented by the variance of the output operator defined as [55]

$$\langle(\Delta a_{\rm out})^2\rangle = \langle a_{\rm out}^\dagger a_{\rm out}\rangle - \langle a_{\rm out}^\dagger\rangle\langle a_{\rm out}\rangle. \tag{22}$$

Under the condition of the nonlinear CPA, the variance of the output operator becomes

$$\langle(\Delta a_{\rm out})^2\rangle = a_{\rm in}^2\frac{\kappa\Delta - \Gamma\delta}{\kappa\Delta + \Gamma\delta}. \tag{23}$$

The nonzero value of the variance is a significant quantum feature. In the linear regime [37], the condition of CPA is $\kappa\Delta = \Gamma\delta$, which corresponds to zero value of variance. However, the condition of $\kappa\Delta = \Gamma\delta$ is unacceptable in the quantum nonlinear regime, for the input field $a_{\rm in}$ in Eq. (14) is equal to zero, which means no input field. To interpret the inconsistency, the linear regime can be treated as an approximation based on the nonlinear regime, where the excitation $\rho_{22} = 0$, the variance of the output field is also zero, and the input field $a_{\rm in}$ is required to be small enough to be approximately ignored. More accurately, in the quantum nonlinear regime, the excitation is nonzero under the CPA condition, i.e., $\kappa\Delta > \Gamma\delta$, and thus the variance of the output operator is also nonzero. The mean photon flux of the output could not be perfectly absorbed and can be detected in the quantum regime. In this sense, it is impossible to realized quantum CPA in the nonlinear quantum systems because of nonzero mean photon flux of the output field, since the ideal CPA requires that both the coherent component and photon number flux are zero. But in the semiclassical treatment where only the coherent component of the output field is eliminated, semiclassical CPA is still realizable in the quantum nonlinear regime.

Moreover, the higher-order correlation can also manifest the nonlinearity in the quantum regime. Under the CPA condition, we calculate the equal-time n-photon correlation function $g^{(n)}(0)$ of the output field,

$$g^{(n)}(0) = \frac{\langle a_{\rm out}^{\dagger n} a_{\rm out}^n\rangle}{\langle a_{\rm out}^\dagger a_{\rm out}\rangle^n}, \tag{24}$$

with the mean output photon flux

$$\langle N_{\rm out}\rangle = \langle a_{\rm out}^\dagger a_{\rm out}\rangle = a_{\rm in}^2\frac{\kappa\Delta - \Gamma\delta}{\kappa\Delta + \Gamma\delta}. \tag{25}$$

With of the input-output relation Eq. (4), the higher-order correlation becomes

$$\begin{aligned}\langle a_{\rm out}^{\dagger n} a_{\rm out}^n\rangle &= \langle (n a_{\rm in}^{n-1}\sqrt{T}a^\dagger - a_{\rm in}^n)(n a_{\rm in}^{n-1}\sqrt{T}a - a_{\rm in}^n)\rangle \\ &= a_{\rm in}^{2n}\left[n^2\frac{\kappa\Delta - \Gamma\delta}{\kappa\Delta + \Gamma\delta} + (n-1)^2\right],\end{aligned} \tag{26}$$

after neglecting the two- and more-photon correlations of the intracavity field due to the truncation of the higher-order polariton states via the photon blockade. The equal-time n-photon correlation functions $g^{(n)}(0)$ are

$$g^{(n)}(0) = \left(\frac{\kappa\Delta + \Gamma\delta}{\kappa\Delta - \Gamma\delta}\right)^n\left[(n-1)^2 + n^2\frac{\kappa\Delta - \Gamma\delta}{\kappa\Delta + \Gamma\delta}\right]. \tag{27}$$

Different from the linear CPA [56], the quantum state of nonlinear CPA is the superposition of the photon state $|0\rangle$ and $|1\rangle$, a coherent superposition state with certain purity. $g^{(n)}(0) > 1$ is fulfilled in the nonlinear CPA, and the photons tend to bunch, i.e., $g^{(2)}(0) = 21$, $g^{(3)}(0) = 117$, with the parameters used in Fig. 6 ($\kappa = 2/3\Gamma$, $g = 20/3\Gamma$, $T = 0.01$, and $a_{\rm in} = 0.0265$), which shows the nonlinear processes with the strong multiphoton correlations. In addition, the result is distinct from the sub-Poissonian statistics of the output field in the typical photon blockade experiment [41], where the statistics of the output field are the same as the intracavity field due to the vacuum input field at the output port. Here, the state at the output field is the superposition of the mixed and antibunching state of the intracavity field and the input coherent state, and moreover, the superposition should guarantee the zero of mean value of the output field. Thus the input field should take the explicit value determined in Eq. (14), and the zero value of the average amplitude of the output field increases multiphoton correlations. Therefore the quantum nonlinear CPA produces an exotic photon distribution in the quantum sense, although the classical (mean) value of the output is zero.

V. CONCLUSION

To conclude, we present a study of CPA phenomenon in a nonlinear quantum CQED system, where the emitter single

atom and cavity mode is strongly coupled, and the polariton excitation is confined within one excitation due to the photon blockade effect. The output field is nonlinearly related to the input field, and the CPA is still achievable at a given input field strength when the frequency of the input laser fields matches the frequency of the polariton transition. However, the incoherent processes, such as atomic and cavity dissipations, will reduce the coherence of the intracavity field, which leads to the incomplete destructive interference with the input fields. Via analyzing the purity of the intracavity field, we find that there exists a lower limit for the purity below which the CPA is not possible. Moreover, we find that the intracavity field is always quadrature squeezed under the CPA condition: a better squeezing occurs when the cavity field frequency is blue-detuned relative to the atomic transition frequency, in which the photonic excitation contributes more to the polariton excitation. Finally, the distinction between the quantum linear CPA analysis and the semiclassical nonlinear CPA analysis is presented from the variance of the output field and its higher-order correlation functions. Statistically, the CPA in a quantum nonlinear system is realizable with a null value of the average output field.

ACKNOWLEDGMENT

This work is supported by the National Natural Science Foundation of China (Grants No. 11474119, No. 11774118, and No. 11504031).

[1] Y. D. Chong, L. Ge, H. Cao, and A. D. Stone, Phys. Rev. Lett. **105**, 053901 (2010).
[2] W. Wan, Y. Chong, L. Ge, H. Noh, A. D. Stone, and H. Cao, Science **331**, 889 (2011).
[3] L. Zhou, Z. R. Gong, Y. Liu, C. P. Sun, and F. Nori, Phys. Rev. Lett. **101**, 100501 (2008).
[4] D. S. Wiersma, P. Bartolini, Ad Lagendijk, and R. Righini, Nature (London) **390**, 671 (1997).
[5] M. Stözer, P. Gross, C. M. Aegerter, and G. Maret, Phys. Rev. Lett. **96**, 063904 (2006).
[6] P. Wei, C. Croënne, S. T. Chu, and J. Li, Appl. Phys. Lett. **104**, 121902 (2014).
[7] S. Dutta-Gupta, O. J. F. Martin, S. D. Gupta, and G. S. Agarwal, Opt. Express **20**, 1330 (2012).
[8] T. Y. Kim, M. A. Badsha, J. Yoon, S. Y. Lee, Y. C. Jun, and C. K. Hwangbo, Sci. Rep. **6**, 22941 (2016).
[9] S. Dutta-Gupta, R. Deshmukh, A. V. Gopal, O. J. F. Martin, and S. D. Gupta, Opt. Lett. **37**, 4452 (2012).
[10] T. Roger, S. Vezzoli, E. Bolduc, J. Valente, J. J. F. Heitz, J. Jeffers, C. Soci, J. Leach, C. Couteau, N. I. Zheludev, and D. Faccio, Nat. Commun. **6**, 7031 (2014).
[11] J. Yoon, M. Zhou, Md. A. Badsha, T. Y. Kim, Y. C. Jun, and C. K. Hwangbo, Sci. Rep. **5**, 12788 (2015).
[12] A. L. Fannin, J. W. Yoon, B. R. Wenner, J. W. Allen, M. S. Allen, and R. Magnusson, IEEE Photon. J. **8**, 6802307 (2016).
[13] A. Mostafazadeh and M. Sarisaman, Phys. Rev. A **91**, 043804 (2015).
[14] P. Bai, K. Ding, G. Wang, J. Luo, Z. Q. Zhang, C. T. Chan, Y. Wu, and Y. Lai, Phys. Rev. A **94**, 063841 (2016).
[15] S. Feng and K. Halterman, Phys. Rev. B **86**, 165103 (2012).
[16] G. Nie, Q. Shi, Z. Zhu, and J. Shi, Appl. Phys. Lett. **105**, 201909 (2014).
[17] M. Papaioannou, E. Plum, J. Valente, E. T. F. Rogers, and N. I. Zheludev, APL Photonics **1**, 090801 (2016).
[18] X. Hu, S. Yuan, A. Armghan, Y. Liu, C. Zeng, Z. Jiao, H. Lv, Y. Huang, Q. Huang, Y. Wang, and J. Xia, J. Opt. **18**, 125101 (2016).
[19] H. Park, S. Lee, J. Kim, B. Lee, and H. Kim, Opt. Express **23**, 24464 (2015).
[20] S. Mukherjee and S. D. Gupta, Eur. Phys. J. Appl. Phys. **76**, 30001 (2016).
[21] J. Zhang, C. Guo, K. Liu, Z. Zhu, W. Ye, X. Yuan, and S. Qin, Opt. Express **22**, 012524 (2014).
[22] X. Hu and J. Wang, Opt. Lett. **40**, 5538 (2015).
[23] N. Kakenov, O. Balci, T. Takan, V. A. Ozkan, H. Altan, and C. Kocabas, ACS Photonics **3**, 1531 (2016).
[24] F. Liu, Y. D. Chong, S. Adam, and M. Polini, 2D Materials **1**, 031001 (2014).
[25] M. L. Villinger, M. Bayat, L. N. Pye, and A. F. Abouraddy, Opt. Lett. **40**, 5550 (2015).
[26] S. Longhi, Opt. Lett. **40**, 1278 (2015).
[27] L. Baldacci, S. Zanotto, and A. Tredicucci, Rend. Fis. Acc. Lincei **26**, 219 (2015).
[28] A. Sinha and R. Roychoudhury, Int. J. Theor. Phys. **54**, 3991 (2015).
[29] J. Wu, M. Artoni, and G. C. La Rocca, Sci. Rep. **6**, 35356 (2016).
[30] J. M. Rothenberg, C. P. Chen, J. J. Ackert, J. I. Dadap, A. P. Knights, K. Bergman, R. M. Osgood, Jr., and R. R. Grote, Opt. Lett. **41**, 2537 (2016).
[31] A. Mostafazadeh and M. Sarisaman, Proc. R. Soc. London, Ser. A **468**, 3224 (2012).
[32] H. Li, S. Suwunnarat, R. Fleischmann, H. Schanz, and T. Kottos, Phys. Rev. Lett. **118**, 044101 (2017).
[33] N. Trautmann, G. Alber, and G. Leuchs, Phys. Rev. A **94**, 033832 (2016).
[34] S. Zanotto and A. Melloni, J. Appl. Phys. **119**, 163103 (2016).
[35] V. Achilleos, O. Richoux, and G. Theocharis, J. Acoust. Soc. Am. **140**, EL94 (2016).
[36] K. Nireekshan Reddy and S. Dutta Gupta, Bulletin of PFUR, Series Mathematics, Information Sciences Physics **4**, 112 (2014).
[37] G. S. Agarwal and Y. Zhu, Phys. Rev. A **92**, 023824 (2015).
[38] G. S. Agarwal, K. Di, L. Wang, and Y. Zhu, Phys. Rev. A **93**, 063805 (2016).
[39] L. Wang, K. Di, Y. Zhu, and G. S. Agarwal, Phys. Rev. A **95**, 013841 (2017).
[40] S. Rebić, A. S. Parkins, and S. M. Tan, Phys. Rev. A **65**, 063804 (2002).
[41] K. M. Birnbaum, A. Boca, R. Miller, A. D. Boozer, T. E. Northup, and H. J. Kimble, Nature (London) **436**, 87 (2005).
[42] C. Hamsen, K. N. Tobazzi, T. Wilk, and G. Rempe, Phys. Rev. Lett. **118**, 133604 (2017).
[43] L. Tian and H. J. Carmichael, Phys. Rev. A **46**, 6801(R) (1992).
[44] A. D. Stone, Phys. Today **64**(11), 68 (2011).

[45] M. Mücke, J. Bochmann, C. Hahn, A. Neuzner, C. Nölleke, A. Reiserer, G. Rempe, and S. Ritter, Phys. Rev. A **87**, 063805 (2013).
[46] M. Keller, B. Lange, K. Hayaska, W. Lange, and H. Walther, Nature (London) **431**, 1075 (2004).
[47] K. Hennessy, A. Badolato, M. Winger, D. Cerace, M. Atatüre, S. Gulde, S. Fält, E. L. Hu, and A. Imamoğlu, Nature (London) **445**, 896 (2007).
[48] C. Kurtsiefer, S. Mayer, P. Zarda, and H. Weinfurter, Phys. Rev. Lett. **85**, 290 (2000).
[49] K. Wódkiewicz, P. L. Knight, S. J. Buckle, and S. M. Barnett, Phys. Rev. A **35**, 2567 (1987).
[50] G. Li and J. Peng, *Introduction to Modern Quantum Optics* (World Scientific, Singapore, 1998).
[51] P. Bertet, A. Auffeves, P. Maioli, S. Osnaghi, T. Meunier, M. Brune, J. M. Raimond, and S. Haroche, Phys. Rev. Lett. **89**, 200402 (2002).
[52] W. Wang, L. Hu, Y. Xu, K. Liu, Y. Ma, S.-B. Zheng, R. Vijay, Y. P. Song, L.-M. Duan, and L. Sun, Phys. Rev. Lett. **118**, 223604 (2017).
[53] D. F. Walls and P. Zoller, Phys. Rev. Lett. **47**, 709 (1981).
[54] C. H. H. Schulte, J. Hansom, A. E. Jones, C. Matthiesen, C. L. Gall, and M. Atatüre, Nature (London) **525**, 222 (2015).
[55] I. Urizar-Lanz and G. Tóth, Phys. Rev. A **81**, 052108 (2010).
[56] Y. D. Chong, H. Cao, and A. D. Stone, Phys. Rev. A **87**, 013843 (2013).